Analytical Calculation Model for Mach Wave Parameters

Zhu Chuansheng(朱传胜)[1], *Huang Zhengxiang*(黄正祥)[1*],
Liu Rongzhong(刘荣忠)[1], *Ji Long*(姬龙)[2]

1. School of Mechanical Engineering, Nanjing University of Science and Technology, Nanjing, 210094, P. R. China;
2. No. 203 Research Institute of China Ordnance Industries, Xi'an, 710065, P. R. China)

(Received 4 November 2013; revised 24 May 2014; accepted 25 June 2014)

Abstract: When a wave shaper is embedded in a liner, Mach wave will emerge above the liner, which affects the head shape of an explosively formed projectile. Mach wave parameters, including radius and pressure need to be determined to effectively match Mach wave with the liner, so that a good head shape can be obtained. An analytical calculation model for Mach wave parameter is presented based on three-shock theory, and the theoretical values agree well with the experimental ones. The analysis shows that when the radius of the wave shaper is constant, the radius of the Mach wave increases, whereas the pressure decreases while increasing the distance between the liner and the wave shaper. When the distance between the liner and the wave shaper is constant, the radius of the Mach wave increases, whereas the pressure decreases when decreasing the radius of the wave shaper.

Key words: explosion mechanism; explosively formed projectile (EFP); wave shaper; Mach wave

CLC number: O389; TJ410.3 **Document code**: A **Article ID**: 1005-1120(2014)06-0688-05

1 Introduction

Explosively formed projectile (EFP) is used in numerous modern ammunition systems for its many advantages, including effective stand-off and high secondary effects after penetration. Designers are often confronted by a problem that the wave shaper should be embedded in charge passively, for example, sensing elements have to be embedded in charge to decrease the length of the warhead in many smart ammunition systems. Thus, the wave shaper has to be embedded in charge to clothe these sensing elements[1]. In addition, the wave shaper can be embedded in charge actively, such that the velocity of the penetrator can be increased because of detonation wave shaping by using the wave shaper[2-5]. However, the Mach wave may emerge above the liner as a wave shaper is embedded in charge, which affects the head shape of EFP. If the radius of a wave shaper is large, the pressure behind the Mach wave is twice to thrice the pressure behind the detonation wave, thus resulting in a poor head shape of EFP because of the unreasonable matching relation between the Mach wave and the liner. The poor head shape decreases the penetration performance of EFP[6-7].

The pressure behind the Mach wave decreases from 4 times the CJ pressure to normal CJ pressure with an increasing incident angle[5]. Since the pressure behind the Mach wave is related to the incident angle of the detonation wave, the pressure and the radius can be controlled by changing the wave shaper diameter and the distance between the wave shaper and the liner which determine the incident angle at the top of liner.

Mach wave parameters, such as radius and pressure, need to be calculated to control the relation between the Mach wave and the liner. A good head shape can then be obtained. An analytical caculation model for Mach wave parameters is presented based on three-shock theory to calculate the growth angle, the radius, the velocity along the plane of symmetry, and the pressure.

* **Corresponding author**: Huang Zhengxiang, Professor, E-mail: huangyu@mail.njust.edu.cn.

2 Analytical Calculation Model for Mach Wave Parameters

When two detonation waves collide, regular reflection is first observed. If the incident angle ψ_I is larger than the critical angle ψ_{IC}, Mach reflection will occur. Fig. 1 represents the geometry of the classical Mach reflection analysis. The symmetry plane of the colliding detonation waves is represented as a perfectly rigid wall. The most basic analysis is to estimate the flow as the intersection of two plane waves that are tangent to the detonation fronts.

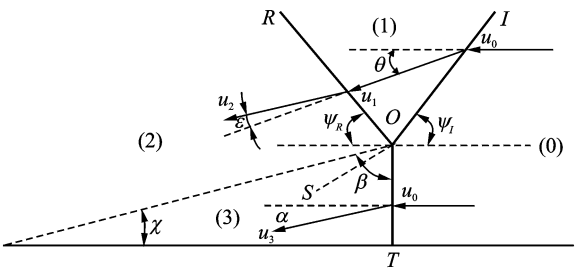

Fig. 1 Flow setup of Mach reflection

As Fig. 1 shows, OI is the wave front of the incident detonation, OR the wave front of the reflected shock, O the triple point, and T the collision point, u_0, u_1, u_2, and u_3 are the particle velocity in zone (0), (1), (2), and (3), respectively. The image can be separated into four regions by the detonation and shock waves: zone (0) is unreacted explosive; zone (1) is the region behind the detonation wave; zone (2) is the region behind the reflection wave; and zone (3) is the region behind the Mach wave[8-9]. The parameters of each zone are shown with the corresponding subscript. Based on the descriptions of detonation reflection in explosion[10], the parameters of each region are described as follows:

Mach number Ma_1 and the deflection angle θ in region (1) are defined by[10]

$$\begin{aligned} Ma_1 &= \sqrt{1+\left(\frac{\gamma+1}{\gamma}\right)^2\cot^2\psi_I} \\ \theta &= \arctan\left[\frac{\tan\psi_I}{1+\gamma(1+\tan^2\psi_I)}\right] \end{aligned} \tag{1}$$

where γ is the exponent in the polytropic equation of state for the explosion.

In region (2), based on equations of mass, momentum, and energy conservation, the following equation is obtained[10]

$$\begin{aligned} \frac{P_2}{P_{CJ}} &= \frac{2\gamma}{\gamma+1}Ma_1^2\sin^2(\psi_R+\theta)-\frac{\gamma-1}{\gamma+1} \\ \frac{\rho_2}{\rho_{CJ}} &= \frac{(\gamma+1)Ma_1^2\sin^2(\psi_R+\theta)}{(\gamma-1)Ma_1^2\sin^2(\psi_R+\theta)+2} \\ \tan\varepsilon &= \frac{[Ma_1^2\sin^2(\psi_R+\theta)-1]\cot(\psi_R+\theta)}{Ma_1^2\left[\frac{\gamma+1}{\gamma}-\sin^2(\psi_R+\theta)\right]+1} \end{aligned} \tag{2}$$

where P_{CJ} and ρ_{CJ} are the CJ detonation pressure and the density of the explosive, respectively; and ε the deflection angle.

In region (3), based on the equations of mass, momentum, and energy conservation, the following equation is derived[10]

$$\begin{aligned} \frac{D_M}{D_{CJ}} &= \frac{\sin\beta}{\sin\psi_I} \\ \frac{P_3}{P_{CJ}} &= \frac{\sin^2\beta}{\sin^2\psi_I}\left(1+\sqrt{1-\frac{\eta\sin^2\psi_I}{\sin^2\beta}}\right) \\ \frac{\rho_0}{\rho_3} &= \frac{1}{\gamma+1}\left(\gamma-\sqrt{1-\frac{\eta\sin^2\psi_I}{\sin^2\beta}}\right) \\ \tan\alpha &= \frac{(1-\rho_0/\rho_3)\tan\beta}{1+(\rho_0/\rho_3)\tan^2\beta} \end{aligned} \tag{3}$$

where D_M and D_{CJ} are the velocity of the Mach wave and detonation wave, respectively, ρ_0 is the initial density of the explosion, β the angle of the tangent line at the Mach wave to the symmetry axis, η the ratio of the specific chemical energy release of the explosive material that passes through the Mach wave to that of the material going through CJ detonation front, and α the deflection angle.

The medium in regions (2) and (3) can meet the conditions that the flow velocity is parallel and the pressures are equal, that is[11]

$$\begin{aligned} P_2 &= P_3 \\ \varepsilon+\alpha &= \theta \end{aligned} \tag{4}$$

We can obtain the parameters of P_3, β, and α near the triple point by solving Eqs. (1-3). The growth angle of the Mach wave χ can be obtained[11] as follows

$$\chi = \frac{\pi}{2}-\beta \tag{5}$$

According to Lambourn[12] and Hull[13], the values of χ obtained from Eq. (5) are significantly greater than the experimental values because the straight Mach wave assumption is used. Based on the experimental values reported by Lambourn[12], the theoretical value χ can be modified as

$$\chi_M = \frac{\chi}{-0.009\ 9\psi_I^2 + 1.295\psi_I - 38.347\ 1} \quad (6)$$

where χ_M, χ and ψ_I are the degree values.

An analytical calculation model for Mach wave radius can be proposed when the growth angle of the Mach wave χ_M is obtained.

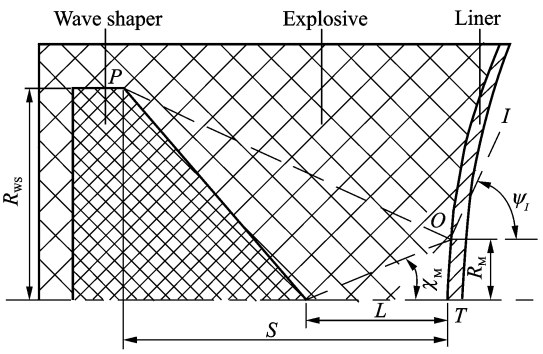

Fig. 2 Calculation schematic of Mach wave radius

As shown schematically in Fig. 2, OI is the incident detonation front, O the triple point, T the collision point, P the edge of the wave shaper, R_{WS} the radius of the wave shaper, S the distance between the liner and wave shaper. ψ_I, R_M, χ_M, and L represent the incident angle of detonation wave, the radius of the Mach wave, the growth angle of the Mach wave, and the distance from starting point of the Mach wave to the liner, respectively. The starting point of the Mach wave is generally at the place where the incident angle of detonation wave is 41°[12], such that L can be calculated geometrically.

According to the mathematical description in Fig. 2, R_M can be calculated as

$$\tan\psi_I = \frac{S}{R_{WS} - R_M} \qquad (7)$$
$$R_M = L\tan(\chi_M)$$

The velocity of the Mach wave along the plane of symmetry D_M and pressure P_3 of the Mach wave can be calculated using Eq. (3).

3 Comparison Between Theory and Experiment

Lambourn and Wright[12] obtained the change curve of χ and D_M along with ψ_I in the Composition B charge. The experimental values of χ are plotted against ψ_I in Fig. 3 along with the theoretical and modified values. Moreover, the values D_M/D_{CJ} derived from the experimental results are plotted against ψ_I in Fig. 4 along with the theoretical values.

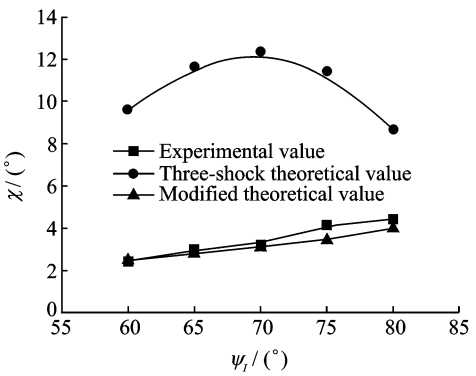

Fig. 3 Growth angle of Mach wave v. s. incident angle

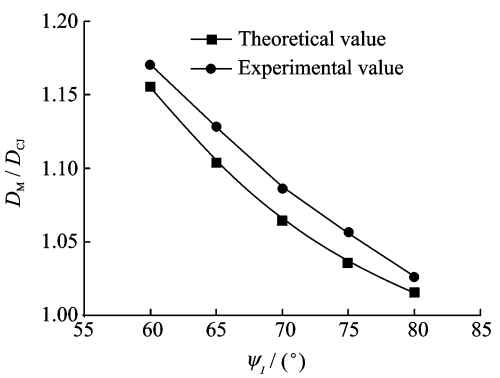

Fig. 4 Velocity of Mach wave v. s. incident angle

As shown in Fig. 3, the three shock theoretical values are significantly greater than the experimental values because the three-shock theory ignores the influence of the rarefaction wave behind the Mach wave. The modified theoretical values seem to agree well with experimental ones. A comparison between the theoretical and the experimental values in Fig. 4 indicates that the theoretical D_M/D_{CJ} are highly accurate and the errors

do not exceed 2%.

Hull[13] studied the Mach reflection of spherical detonation waves and measured the radiuses of the Mach wave of PBX 9501 and PBX 9502 as well as the pressure behind the Mach wave of PBX 9501. Fig. 5 shows a radius comparison between the theory and the one measured from the experiments, both for PBX 9501 and PBX 9502. Fig. 6 shows a comparison between the pressure behind the Mach wave calculated by the theory and measured for PBX 9501.

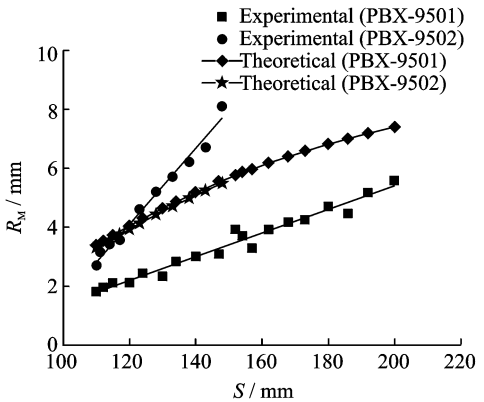

Fig. 5 Radius v. s. displacement of the Mach wave

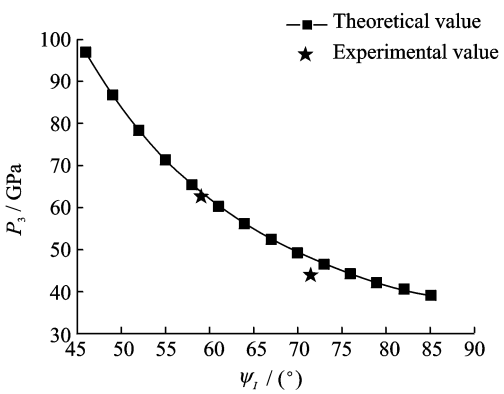

Fig. 6 Pressure behind the Mach wave v. s. incident angle

As shown in Fig. 5, the theoretical R_M fails to replicate the experimental values accurately for PBX 9501 and PBX 9502. The inconsistency is caused by two reasons. One is that explosive properties, such as reaction zone[13] and the value of η[8], can affect the growth angle of the Mach wave. However, the analytical model does not include these explosive properties. Therefore, the theoretical values of R_M are approximately the same with those of PBX 9501 and PBX 9502, but the experimental values of R_M are significantly different. The other is that errors exist in the experimental values. The critical angles of the Mach reflection calculated from experimental values in PBX 9501 and PBX 9502 are 56° and 63°, respectively, which are evidently overestimated[8,13], because the configuration of the Mach wave is highly complex, which makes the accurate determination of the triple point difficult, thereby leading to reading errors. A comparison between the theoretical and experimental values from Fig. 6 indicates that the theoretical pressure behind the Mach wave is accurate, and the errors at two experimental points are 1.7% and 8.6%.

As Fig. 5 shows, when the radius of the wave shaper R_{WS} is constant, the radius of the Mach wave R_M increases with increasing displacement from the Mach wave front to initiation. As shown in Fig. 6, the pressure behind the Mach wave P_3 decreases with the increasing incident angle of the detonation wave ψ_I. As Fig. 2 indicates, when the radius of the wave shaper R_{WS} is constant, both L and ψ_I increase with increasing distance between the liner and wave shaper S. When S is constant, both L and ψ_I increase with increasing radius of the wave shaper R_{WS}.

4 Conclusions

Based on the preceding analysis, two conclusions can be drawn: (1) When the radius of the wave shaper R_{WS} is constant, we can increase the radius of the Mach wave and decrease the pressure behind the Mach wave by increasing the distance between the liner and wave shaper S; and (2) when the distance between the liner and wave shaper S is constant, we can increase the radius of the Mach wave and decrease the pressure behind the Mach wave by decreasing the radius of the wave shaper R_{WS}.

References:

[1] Men Jianbing, Jiang Jianwei, Luo jian. Numerical simulation research on the influence of sensing elements on EFP forming [J]. Journal of Ballistics,

2005,17(1):67-71. (in Chinese)

[2] Weimann K. Research and development in the area of explosively formed projectiles charge technology[J]. Propellants, Explosives, Pyrotechnics, 1993, 18(5): 294-298.

[3] Huang Zhengxiang. Mechanism study on jetting projectile charge formation[D]. Nanjing: Nanjing University of Science and Technology, 2003. (in Chinese)

[4] Zhang Xianfeng, Chen Huiwu, Zhao Youshou. Study on shaped charge technique of small diameter which have high velocity EFP[J]. Journal of Projectiles, Rockets, Missiles and Guidance, 2003, 23(3): 107-109. (in Chinese)

[5] Zhang Yanguo, Zhang Xianfeng, He Yong, et al. Detonation wave propagation in shaped charges with large wave-shaper[C]//27th International Symposium on Ballistics. Freiburg, Germany: DEStech Pubcications, 2013:770-782.

[6] Bender D, Fong R, Ng W, et al. Dual mode warhead technology for future smart munitions[C]//19th International Symposium on Ballistics. Interlaken, Switzerland: [s. n.], 2001:679-684.

[7] Fong R, Ng W, Weimann K. Nonaxisymmetric waveshaped EFP warheads[C]//20th International Symposium on Ballistics. Orlando, FL, USA: DE Stech Pubcications, 2002:582-588.

[8] Dunne B. Mach reflection of detonation waves in condensed high explosives Ⅱ[J]. The Physics of Fluids, 1964, 7(10), 1707.

[9] Zhang Xianfeng, Huang Zhengxiang, Qiao Liang. Detonation wave propagation in double-layer cylindrical high explosive charges[J]. Propellants, Explosives, Pyrotechnics, 2011, 36(3):210-218.

[10] Cao Bing. Study on the phenomenon of charge detonation and EFP formation under the condition of multi-point ignition at the upper end of the charge [D]. Nanjing: Nanjing University of Science and Technology, 1998. (in Chinese)

[11] Wang Jihai. Two-dimensional nonsteady flow and shock waves[M]. Beijing: Science Press, 1994. (in Chinese)

[12] Lambourn B D, Wright P W. Mach interaction of two plane detonation waves[C]//4th International Detonation Symposium. Arlington, USA: U. S. Naval Ordnance Laboratory, 1965:142-152.

[13] Hull L M. Mach reflection of spherical detonation waves[C]//10th International Detonation Symposium. Boston, Massachusetts: U. S. Naval Ordnance Laboratory, 1993:11-18.

(Executive editor: Zhang Bei)